ELSEVIER

Journal of Photochemistry and Photobiology A: Chemistry 113 (1998) 257–264

Journal of Photochemistry and Photobiology A:Chemistry

Photocatalytic degradation of organic dyes in aqueous solution with TiO_2 nanoparticles immobilized on foamed polyethylene sheet

Subrata Naskar, S. Arumugom Pillay, Manas Chanda *

Department of Chemical Engineering, Indian Institute of Science, Bangalore, India

Accepted 27 August 1997

Abstract

Degussa TiO_2 nanoparticles have been immobilized on a foamed polyethylene by thermal bonding to produce a stable catalyst sheet containing 0.7 mg TiO_2 cm^{-2} and retaining 40–50% of active surface area of the particles. On such a catalyst sheet, exposed to radiation of a 125 W mercury vapour lamp, decomposition of about 0.3 mg of methylene blue (MB) is obtained per cm^2 in 1 h at ambient temperature from an aqueous solution of 200 ppm MB. The rate data fit well to classical Langmuir–Hinshelwood (L–H) rate form. This rate form also results from mechanisms based on the assumption of hydroxyl radical formation on the irradiated catalyst and a reaction between the hydroxyl radical and the organic dye molecule, either or none of them being adsorbed on the catalyst surface. An activation energy of 14.5 kcal mol^{-1} is obtained for the photocatalytic decomposition of methylene blue following the L–H rate laws.

Keywords: Photocatalytic degradation; Titania; Methylene blue; Polyethylene

1. Introduction

In recent years, photocatalytic degradation has attracted increasing attention as a promising method for the removal of toxic organic and inorganic contaminants from water [1–5]. However, despite its promise, the development of a practical treatment system based on heterogeneous photocatalysis has not yet been successfully achieved, because there are many operational parameters which must be considered. In particular, the success of photocatalytic degradation in wastewater treatment will depend on how much energy costs can be brought down. This can be achieved by (1) improving photocatalytic degradation efficiency such as by catalytic modification and optimization of process conditions, and (2) designing a low-cost reactor for continuous treatment of wastewater using solar radiation.

A practical limitation in the use of a solar reactor for photodegradation is separation of the catalyst. Since it is difficult to separate the fine TiO_2 powder catalyst from the treated wastewater by any simple operation, the development of a viable solar reactor will hinge, to a large extent, on the degree of success that can be achieved in immobilizing the powder catalyst on a support in such a way as to afford a reasonably high surface area and accessibility of the immobilized catalyst. Several methods of supporting the catalyst on a substrate have been reported [6–8].

In the present article, we present a method of immobilizing TiO_2 powder on a foamed polyethylene sheet by controlled fusion bonding that affords a relatively high degree of loading of the catalyst on the surface. The TiO_2 immobilized in this way is found to be photocatalytically active, capable of decomposing a variety of organic substances including carboxylic acids, alcohols, phenols and amines. In this work, we however focus on the degradation of organic dyes, as dyes constitute more complex entities and present a significant challenge to environmental chemists because of the persistent environmental health risks. The efficacy of the use of TiO_2 particulate suspension for the photooxidation of the organic dye, methylene blue, has been demonstrated [9]. In general, however, study of photocatalytic degradation of organic dyes has been largely neglected. This prompted us to undertake the present investigation.

The work presented here is part of a systematic kinetic study on TiO_2-mediated photooxidation of synthetic organic dyes using surface-immobilized TiO_2. The effects of parameters, such as pH, initial dye concentration, catalyst loading and temperature, are examined, taking methylene blue as a specific dye for analysis. The photocatalytic degradation obtained in sunlight has been compared with that obtained by irradiation with mercury vapour lamp using the same immobilized TiO_2 catalyst.

* Corresponding author. Tel.: +91-80-3092341; fax: +91-80-3342085; e-mail: chanda@chemeng.iisc.ernet.in

1010-6030/98/$19.00
PII S1010-6030(97)00258-X

2. Experimental details

2.1. Chemicals

Titanium dioxide was Degussa P-25 (average particle size of 30 nm and BET surface area of 50 ± 15 $m^2 g^{-1}$; consisting [10] of 99.5% TiO_2 with approximately 80% anatase and 20% rutile). Methylene blue (99%) supplied by Qualigens Fine Chemicals, Bombay, was used as received. Detailed studies were made only with this dye. Other dyes used in the work were obtained from BDH, Glaxo, Lobo-chemie and Merck. These dyes of greater than 90% purity were used only for a set of comparative runs of photocatalysis under solar radiation.

2.2. Catalyst immobilization

Degussa P-25 anatase form of TiO_2 was immobilized on polyethylene film surface by hot pressing as follows. Foamed polyethylene sheet (30 cm × 30 cm and thickness 1.5 mm) was scraped on the surface with a sharp knife for a few minutes and then dipped into 10–15% (by wt.) aqueous suspension of TiO_2 for 10 min. The TiO_2 coated sheet was placed between two aluminium foils and pressed with electrically heated iron adjusted to 70°C. The sheet was again dipped in 10–15% (by wt.) suspension for 5 min and pressed between aluminium foils with hot iron at 70°C. The process was repeated once more and the sheet allowed to dry. After removing the loosely held TiO_2 particles by prolonged and vigorous tapping, the TiO_2 loaded sheet was shaken in a large body of water for a long time till there was no loss of the catalyst particles. The sheet was air dried and stored. The difference in weights of coated and bare polyethylene sheet gave TiO_2 coverage as 6.9×10^{-4} g cm^{-2}. SEM photographs of the coated sheet are shown in Fig. 1 which confirmed the average particle size of immobilized TiO_2 to be about 30 nm.

2.3. Photochemical reactor

Separate photolysis experiments were conducted with TiO_2-coated polyethylene sheet both in the sunlight and in the radiation from a mercury vapour lamp. The solar reactor consisted of a 26 cm diameter and 3.0 cm deep, open stainless steel tray which was mounted on a box housing a variable speed rotor. The TiO_2 coated polyethylene sheet of appropriate diameter was laid on the floor of the tray containing the dye solution. The solution was stirred by a centrally mounted horizontal blade slightly below the liquid surface and sufficiently above the catalyst sheet allowing a gap of about 5 mm. The solution was agitated continuously with full exposure to sunlight from 10 AM to 3 PM. The solar intensity was measured at regular intervals during the course of the runs with a pyranometer which yielded an average value of 0.60 kW m^{-2}. Aliquots of the irradiated samples were collected during the illumination. Two control runs were carried out for each set of experiment. The first involved monitoring the changes in concentration of an identical solution to that being irradiated with catalyst present; this solution was stirred in the presence of the catalyst in the dark. This was carried out to take into account the change in the dye concentration only due to adsorption on the catalyst. The second experiment involved the irradiation of the dye solution in the absence of catalyst to account for any direct photolysis. The solution volume change during experiments due to evaporation loss was corrected by adding the required amount of water.

A photochemical reactor used to study the activity of the coated catalyst sheet in UV radiation consisted of a jacketed quartz tube of 21 cm length and 3.4 cm i.d., holding a 125 W medium pressure mercury vapour lamp and placed in a pyrex glass outer container of diameter 9 cm, containing the dye solution. The lamp radiated predominantly 365–366 nm light with smaller amounts at 265, 297, 303 and 313 nm. A 21.6 cm × 6.5 cm strip of the TiO_2-coated polyethylene sheet was placed securely covering the entire inside wall of the outer glass container. The dye solution contained in the annular

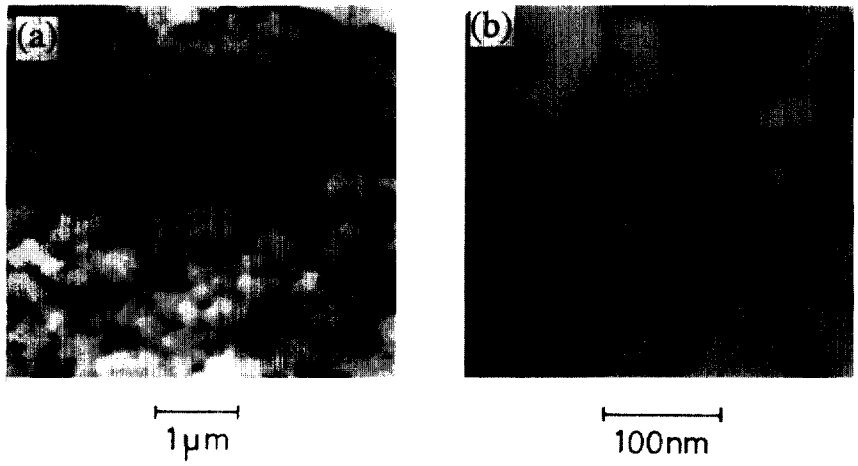

Fig. 1. Scanning electron micrographs of the TiO_2 nanoparticles thermally bonded on foamed polyethylene sheet. Magnification: (a) ×13,000 and (b) ×70,000.

space between the catalyst sheet and the outer surface of the jacketed quartz cylinder was vigorously stirred by a magnetic stirrer, while pure oxygen was bubbled through the solution. Aliquots (5 ml) were retrieved from the reactor and returned to the reactor after analysis.

2.4. Analysis

Most of the dyes show a high molar absorptivity (ϵ) allowing the rate of decomposition to be computed easily by UV measurements even for very dilute solutions. UV spectrophotometry was therefore used for determining the extent of dye degradation produced by photolysis. Absorbances of both the chromophoric groups and aromatic rings in the dye were measured at the respective wavelengths. The extents of decomposition of the chromophores and aromatic rings in the dye molecule were calculated using the Beer–Lambert law from the measured absorbances of the photolysis solution and the corresponding feed solution of known concentration.

Since the UV spectroscopic method of analysis only measured concentrations of chromophoric and aromatic groups and provided no information on the extent of mineralization, a run was conducted in which the aliquots drawn were analysed for COD (Chemical Oxygen Demand). For the determination of COD, a simple sensitive method [11] based on oxidation of the organic compound by dichromate in sulfuric acid medium and spectrophotometric measurement of the resulting Cr(III) was calibrated using standard solutions of the dye in the concentration range employed in the work.

3. Results and discussion

3.1. Activity of immobilized TiO_2

To determine the extent of loss of catalytic activity due to immobilization, photolysis runs were conducted separately with both the TiO_2-coated plastic sheet and a TiO_2 suspension containing the same amount of TiO_2 as affixed to the sheet, using the same photoreactor set-up in both cases. The photocatalytic degradation obtained in the two cases is compared in Fig. 2. The comparison reveals that the method we have adopted for immobilization of TiO_2 on polyethylene results in about 50–60% loss of activity due to partial embedding of TiO_2 grains on the plastic surface.

3.2. Solar photolysis

Experiments were carried to examine the degradation of various dyes under solar radiation, when the catalyst was coated onto a polyethylene sheet. Dye solutions of initial concentrations 10–15 ppm were contained in the tray of the solar reactor. TiO_2 coated polyethylene sheet was kept submerged in the solution (depth 2.2 cm) and exposed to sunlight. The average solar intensity during the period of exposure as measured with a pyranometer was 0.60 kW m^{-2}.

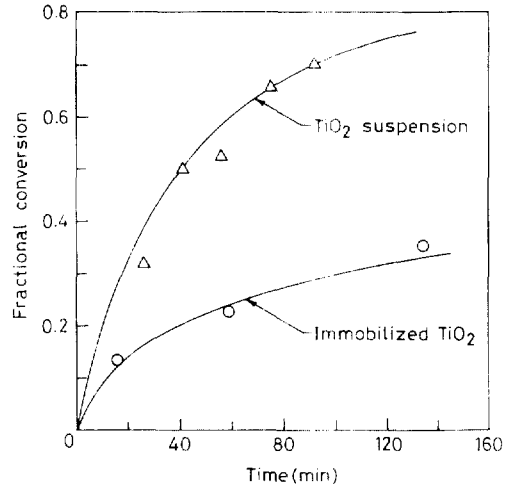

Fig. 2. Comparison of photocatalysis of methylene blue (MB) by TiO_2 suspension and TiO_2 immobilized on polyethylene sheet (21.6 cm × 6.5 cm) both containing 0.097 g TiO_2. MB concentration (initial) 6.25×10^{-4} mol l^{-1}; volume 220 ml; pH 5.72; temperature 26°C; vigorous agitation.

Table 1
Typical data of solar photochemical decomposition[a] of dyes on TiO_2-coated sheet[b]

Dye	Initial conc. (ppm)	Exposure (h)	Decomp. (%)[c]
Methylene blue	20	4	100
Cresol red	10	4	100
Eosin	20	4	100
Crystal violet	30	5	75
Bromocresol purple	30	3	33
Bromothymol blue	50	5	14
Alcian blue	30	4	50
Fuschine	20	3	100

[a]Temperature: 25–28°C, pH: 5–6.
[b]Catalyst loading: 6.9×10^{-4} gm cm^{-2}, volume: 750 ml.
[c]Calculated from decrease in absorbance due to aromatic groups.

The solution was not aerated by bubbling air or stirred. The extent of decomposition of the chromophoric group and of aromatic groups of the dye molecules was measured by UV spectrophotometry. From the data presented in Table 1, it is seen that while all the organic dyes examined undergo photolysis, the susceptibility to photolysis varies from compound to compound and also among groups. In general, aromatic rings are found to be less susceptible to photolysis than chromophoric groups, though both types of groups undergo photolysis.

3.3. Extent of COD removal

The extent of decomposition calculated from a comparison of the UV absorbances does not indicate the degree of mineralization that takes place. To obtain an estimate of mineralization caused by photolysis over TiO_2-coated sheet, aliquots drawn periodically from the reactor were analyzed both by UV spectroscopy to determine the extent of decom-

position of the chromophoric and aromatic groups and by dichromate/sulphuric acid oxidation to determine the reduction of COD. The results obtained for a typical run with methylene blue solution are shown in Fig. 3. As would be expected, the rate of COD reduction by photolysis is less than the rate of decomposition of the dye molecule. It is seen from the data for methylene blue presented in Fig. 3 that photolysis for 2 h produces 34% decomposition of aromatic rings, while COD drops by about 20% in the same period. These results show that TiO_2 supported on the surface of polyethylene is photocatalytically active and suitable for mineralization of an organic dye such as methylene blue.

3.4. Effect of pH

To determine the effect of pH on the rate of photocatalytic degradation of methylene blue, fractional decomposition of the aromatic ring in the dye molecule was monitored by UV absorption as a function of time. The results obtained by such measurements at different pH levels of the dye solution (6.25×10^{-4} mol l^{-1}) are shown in Fig. 4 as the initial rate of aromatic ring decomposition vs. pH. In general, lower pH in the acidic range is seen to enhance the rate of decomposition, the rate at pH 2.0 being about 30% higher than that at pH 6.0. This is indicative of the significant role of the surface properties of the photocatalyst TiO_2. A similar influence of pH on the initial photocatalytic degradation rate of organic compounds has been reported by other workers [12,13].

The pH dependent behaviour can be explained by the effect of pH on both the semiconductor band potentials and the surface dissociation of the hydrated TiO_2. The Nernstian shift of the band edges to more negative values with increase in pH, leads to a decreasing oxidation potential of h_{vb}^+ at high pH [14]. The change in photocatalytic activity may also result from the pH effect on the following dissociation mechanism of TiO_2. The surface of a TiO_2 crystal is covered with TiOH in water:

$$TiOH \rightleftharpoons TiO^- + H^+$$

Since the dissociation does not proceed in acidic solutions [12], the photocatalytic effect is enhanced at a lower pH.

3.5. Effect of concentration

The effect of concentration of methylene blue in aqueous solution on the photocatalytic decomposition rate on immobilized TiO_2 was measured in the UV photocatalytic reactor using a sufficiently high stirring rate at which the stirring rate had no effect on the rate of decomposition of the dye. The results showed that the concentration had a significant effect on the reaction rate, the initial rate increasing with the substrate concentration.

The rate of photocatalytic decomposition of methylene blue also increases significantly with temperature. Typical data for one concentration is shown in Fig. 5 Similar results are also obtained for the other concentrations employed.

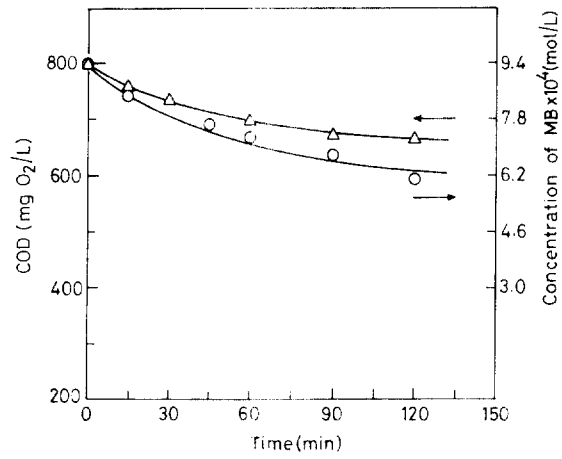

Fig. 3. Comparison of changes in concentration (aromatic groups) and COD of methylene blue (MB) in aqueous solution during photolysis on immobilized TiO_2. Initial concentration of MB 300 ppm; volume 220 ml; pH 6.0; temperature 26°C; TiO_2 (immobilized) 0.097 g.

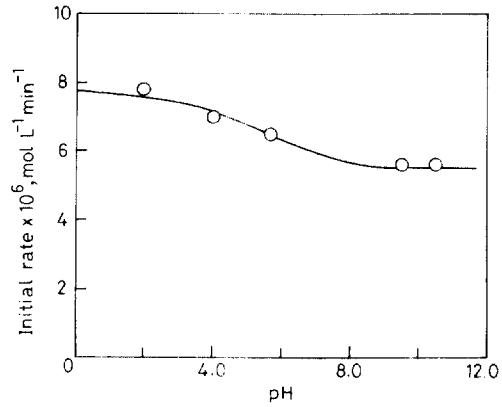

Fig. 4. Effect of pH on initial rate of photolysis of methylene blue (MB) in aqueous solution. MB concentration (initial) 6.25×10^{-4} mol l^{-1}; volume 220 ml; immobilized TiO_2 0.097 g on 21.6 cm × 6.5 cm sheet; temperature 26°C; vigorous agitation.

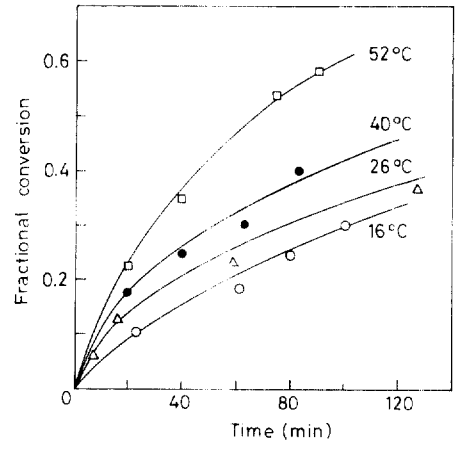

Fig. 5. Effect of temperature on conversion versus time in photolysis of methylene blue (MB) on immobilized TiO_2. Initial concentration of MB 200 ppm (6.25×10^{-4} mol l^{-1}); pH 5.7; volume 220 ml; TiO_2 (immobilized) 0.097 g.

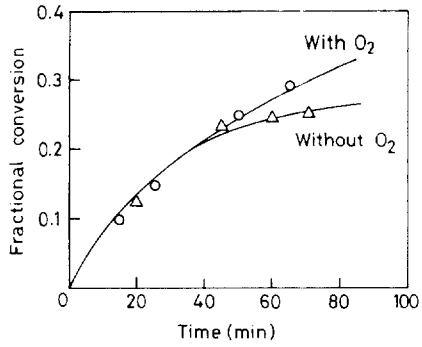

Fig. 6. Effect of dissolved oxygen on photocatalytic decomposition of methylene blue (MB) in aqueous solution by immobilized TiO_2 (0.097 g). MB concentration (initial) 6.25×10^{-4} mol l^{-1}; volume 220 ml; temperature 26°C; vigorous agitation.

3.6. Effect of O_2

Photocatalysis experiments were also carried out in the absence of O_2 (that is, using deaerated water and no external supply of O_2) to compare with the results obtained in the presence of O_2 supplied externally during the run, other conditions being the same. A typical comparison is shown in Fig. 6. It is found that initially (up to 15–20% conversion, depending on the substrate concentration), the rate of oxidation of methylene blue is the same, irrespective of the presence or absence of O_2 in the aqueous solution, while at higher conversion the rate decreases in the absence of external supply of O_2. This result may be indicative of the participation of lattice oxygen in the oxidation process which is taken into account in the kinetic mechanism suggested below.

4. Kinetic analysis

It is well documented that the surface of TiO_2 is readily hydroxylated when the semiconductor is in contact with water [15,16]. Both dissociated and molecular water are bound to the surface. Boehm and Herrmann [17] have estimated that the theoretical maximum surface coverage is 5–15 OH^- nm^{-2}, depending on which crystal plane is considered.

Under near-UV illumination, electron-hole pairs are formed in TiO_2. These two species may recombine in the bulk lattice or migrate to the surface where they can react with adsorbates. Since OH^- and H_2O are the most abundant adsorbates, it is likely that holes will react with these species:

$$l\text{–}OH^- + h^+ \rightleftharpoons l\text{–}\dot{O}H \quad (1)$$

$$l\text{–}H_2O + h^+ \rightleftharpoons l\text{–}\dot{O}H + H^+ \quad (2)$$

where l represents an adsorption site.

In view of the observed fact, as described above, that the oxidation of the organic substrate takes place at a high rate even in the absence of externally supplied O_2 in the initial stages of conversion, it may be postulated that the surface bound OH^- participating in reaction (1) may be available from the following reaction involving lattice oxygen (oxide ion):

$$O_L^{2-} + l + H_2O \rightleftharpoons O_L H^- + l\text{–}OH^-$$

For oxidation of OH^- or H_2O to occur, the oxidation potential for the reactions (1) and (2) must lie above (i.e., be more negative than) the position of the semiconductor valence band, E_v. Since oxidation potentials for the reactions (1) and (2) remain above E_v throughout the entire pH range [18], the oxidation of surface-bound OH^- and H_2O by TiO_2 valence band holes to form $\dot{O}H$ is thermodynamically possible and would be expected under both acidic and basic conditions.

Assuming that the hydroxyl radical, $\dot{O}H$, is the primary oxidant in the photocatalytic system, four possible mechanisms [19] may be suggested for the degradation of organic pollutants in illuminated TiO_2 photocatalyst system, viz., (I) reaction occurs while both $\dot{O}H$ radical and organic molecule are adsorbed; (II) a non-bound $\dot{O}H$ reacts with an adsorbed organic molecule; (III) an adsorbed $\dot{O}H$ radical reacts with a free organic molecule in the liquid phase; and (IV) reaction occurs between two free species in the liquid phase.

A sequence of elementary steps relevant to the derivation of kinetic expressions based on the aforesaid four mechanisms is suggested for the photocatalytic degradation of methylene blue (MB) in the present study:

Excitation:

$$TiO_2 \xrightarrow{h\nu} e^- + h^+ \quad (3)$$

Adsorption:

$$l + MB \underset{k'_{a(MB)}}{\overset{k_{a(MB)}}{\rightleftharpoons}} l\text{–}MB \quad (4)$$

$$\dot{O}H + l \underset{k'_{a(OH)}}{\overset{k_{a(OH)}}{\rightleftharpoons}} l\text{–}\dot{O}H \quad (5)$$

($K_a = k_a/k_a'$ in each case).

Recombination:

$$e^- + h^+ \xrightarrow{k_{rc}} \text{heat} \quad (6)$$

Trapping:

$$l\text{–}OH^- + h^+ \underset{k'_{tr}}{\overset{k_{tr}}{\rightleftharpoons}} l\text{–}\dot{O}H \quad (7)$$

Hydroxyl attack:

Case I

$$l\text{–}\dot{O}H + l\text{–}MB \xrightarrow{k_I} l + l\text{–}Prod \quad (8)$$

Case II

$$\dot{O}H + l\text{–}MB \xrightarrow{k_{II}} l\text{–}Prod \quad (9)$$

Case III

$$l\text{–}\dot{O}H + MB \xrightarrow{k_{III}} l + Prod \quad (10)$$

Case IV

$$\dot{O}H + MB \xrightarrow{k_{IV}} \text{Prod} \qquad (11)$$

The purpose of the above scheme is to reasonably depict the photodegradation process while maintaining enough simplicity to be useful for the development of kinetic equations. Similar rate forms are found in each case, as shown in Appendix AAA. The four kinetic expressions (Table 1) derived are all consistent with reported initial rate and are no more complicated than empirical expressions frequently used to describe photocatalytic degradations.

Reactions (8) through (11) represent four different possible pathways for H attack on the dye, depending on whether the reacting species are on the photocatalyst surface or in the liquid phase. Reaction (9) leads to an adsorbed product and reaction (10) to a liquid-phase product. If the hole-trapping reaction forms a free hydroxyl radical, the conditions represented by reaction (5) differ only by the available diffusion time. In this event, there is no mechanistic difference between cases I and II and between cases III and IV. The rate expressions for case II are derived in Appendix A. Since reactions (3)–(7) remain unchanged for the four cases, all four cases lead to rate laws of a similar form. The algebraic forms of the parameter group (k_g) and (K_g) appearing in the rate laws are summarized in Table 2.

Irrespective of which of the four cases is considered, the expression for k_g is the same (Table 2). Importantly, k_g is predicted to be a function only of catalyst properties and reaction conditions, and therefore, its value should be independent of the particular organic reactant being degraded. The expression for r_{MB} (Table 2) has the appearance of the familiar Langmuir–Hinshelwood kinetic rate law

$$r_i = -\frac{d[MB]}{dt} = \frac{k_i K_i C_i}{1 + K_i C_i} \qquad (12)$$

in the absence of competition from intermediates. Eq. (12) has been employed to describe the observed photocatalytic initial rate results of single-component systems [20–22]. The usual method of obtaining values of the reaction rate constant k_i and the adsorption equilibrium constant K_i is to plot single-component initial rate data as $1/r_i^0$ vs. $1/C_i^0$, where r_i^0 is the initial disappearance rate of reactant i, and C_i^0 is the initial concentration of reactant i. Such a plot should be linear if the L–H rate form (Eq. (12)) is applicable, as predicted by the derived kinetic rate laws (Table 2).

The initial rate data for photocatalytic degradation of methylene blue on immobilized TiO_2 at different temperatures are shown in Fig. 7, plotted as $1/r_0$ vs. $1/[MB]_0$ where $[MB]_0$ is the initial concentration of methylene blue. The linearity of the plots show that L–H (Eq. (12)) is representative of the rate data. The L–H parameters k_{MB} and K_{MB} for methylene blue decomposition obtained from the intercept and slope of the least-squares lines are recorded in Table 3. The Arrhenius plot of k_{MB} (Fig. 8) yields a value of 14.5 kcal mol^{-1} as the activation energy of the photocatalytic decomposition of methylene blue.

Table 2
Derived kinetic rate expressions[a]

$r_{MB} = (k_g K_g [MB])/(1 + K_g [MB])$
$k_g = k_{II}[1 - OH^-]([k_I]/[k_{tr}])^{1/2}$

Case	Description	K_g
I	1-ȮH + 1-MB	$(k_I K_{ad(MB)}[I])/(k'_{tr})$
II	ȮH + 1-MB	$(k_{II} K_{ad(MB)})/(k'_{tr} K_{ad(OH)})$
III	1-ȮH + MB	$(k_{III})/(k'_{tr})$
IV	ȮH + MB	$(k_{IV})/(k'_{tr} K_{ad(OH)}[I])$

[a]See Appendix A.

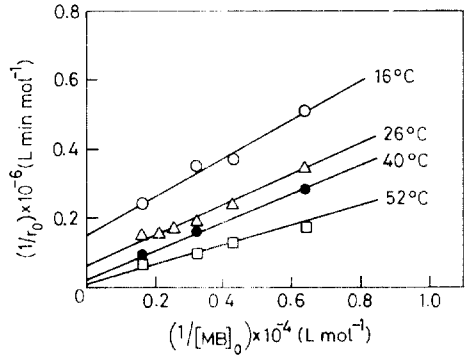

Fig. 7. Plot of (1/rate) on 1/(initial conc.) according to Langmuir–Hinshelwood kinetics.

Table 3
Langmuir–Hinshelwood rate law parameters for photocatalysis of methylene blue on TiO_2

Temperature (°C)	k_{MB} (mol l^{-1} min^{-1})	K_{MB} (l mol^{-1})
16	0.066×10^{-4}	0.278×10^4
26	0.154×10^{-4}	0.147×10^4
40	0.454×10^{-4}	0.065×10^4
52	1.00×10^{-4}	0.036×10^4

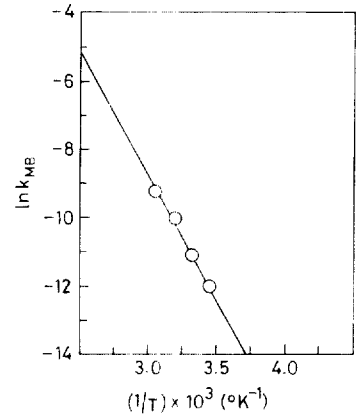

Fig. 8. Arrhenius plot of rate constant (k_{MB}) for methylene blue degradation by photolysis.

5. Conclusions

This work has demonstrated that TiO_2 nanoparticles can be immobilized by thermal bonding on a foamed polyethylene sheet. The resulting catalyst sheet still retains 40–50% of the active surface area as shown by a comparison of the photocatalytic activity of the immobilized TiO_2 with TiO_2 in aqueous suspension under similar conditions of irradiation, solution concentration, temperature and stirring. Many possible mechanisms based on the involvement of hydroxyl radical ($\dot{O}H$) as the primary oxidant in photodecomposition of the organic dye give rise to the Langmuir–Hinshelwood rate form commonly used to describe photocatalytic degradation kinetics. The experimental rate data obtained with different concentrations of the organic dye, methylene blue, fit well to this rate form, yielding an activation energy of 14.5 kcal mol^{-1} for the photodecomposition reaction.

Acknowledgements

The authors thank Professor K.S. Gandhi, Chairman, Chemical Engineering Department, Indian Institute of Science, Bangalore for his interest and the authorities of the Institute for providing facilities for the work.

Appendix A.

We present the derivation of Case I to illustrate the assumptions of the kinetic model. In this scheme, the reactions of interest are Eqs. (3)–(8). For surface reaction control, the rate of disappearance of the organic reactant MB may be represented by

$$r_{MB} = k_1[1-\dot{O}H][1-MB] \quad (A.1)$$

The surface concentrations of $\dot{O}H$ and MB are given by

$$[1-\dot{O}H] = K_{a(OH)}[\dot{O}H][1] \quad (A.2)$$

$$[1-MB] = K_{a(MB)}[MB][1] \quad (A.3)$$

Invoking steady-state approximation for the total concentration of $\dot{O}H$ present:

$$\frac{d[\dot{O}H]}{dt} = k_{tr}[1-OH^-][h^+] - k'_{tr}[1-\dot{O}H] - k_1[1-\dot{O}H][1-MB] = 0 \quad (A.4)$$

Substituting Eq. (A.2) in Eq. (A.4) and solving for $[\dot{O}H]$,

$$[\dot{O}H] = \frac{k_{tr}[1-OH^-][h^+]}{k'_{tr}K_{a(OH)}[1] + k_1K_{a(OH)}[1-MB][1]} \quad (A.5)$$

Similarly, if we use the steady-state approximation for the concentration of holes, we obtain

$$\frac{d[h^+]}{dt} = k_{ex}I - k_{tr}[1-OH^-][h^-] + k'_{tr}[1-\dot{O}H] - k_{rc}[e^-][h^+] = 0 \quad (A.6)$$

Because the photogeneration rates of $[h^+]$ and $[e^-]$ are equal, and because the semiconductor intrinsic carrier density is comparatively low, we may assume $[h^+] = [e^-]$. Therefore,

$$k_{ex}I = k_{tr}[1-OH^-][h^+] - k'_{tr}[1-\dot{O}H] + K_{rc}[h^+]^2 \quad (A.7)$$

Since the rate constant for free carrier recombination (k_{rc}) is much greater than that for hole trapping (k_{tr}) [23], one expects for relatively high $[h^+]$,

$$k_{rc}[h^+]^2 \gg k_{tr}[1-OH^-][h^+] - |k'_{tr}|[1-\dot{O}H] \quad (A.8)$$

under these conditions, Eq. (A.7) simplifies to

$$[h^+] = (k_{ex}I/k_{rc})^{1/2} \quad (A.9)$$

For most photochemical applications, appreciable light intensities are desired. Therefore, one may deal with the situation where Eq. (A.9) describes the illumination dependence. Substitution of Eq. (A.9) into Eq. (A.5) gives

$$[\dot{O}H] = \frac{k_{tr}[1-OH^-](k_{ex}I/k_{rc})^{1/2}}{k'_{tr}K_{a(OH)}[1] + k_1K_{a(OH)}[1-MB][1]} \quad (A.10)$$

Combination of Eqs. (A.1) and (A.2) Eqs. (A.3) and (A.10) then yields

$$r_{MB} = \frac{k_gK_g[MB]}{1+K_g[MB]} \quad (A.11)$$

where

$$k_g = k_{tr}[1-OH^-]\left(\frac{k_{ex}I}{k_{rc}}\right)^{1/2} \quad (A.12)$$

and

$$K_g = \frac{k_1K_a(MB)[1]}{k'_{tr}} \quad (A.13)$$

Rate expressions for the other cases are similarly derived.

References

[1] V.N. Parmov, K.I. Zamarev, in: N. Serpone, E. Pelizzetti (Eds.), Photocatalysis—Fundamentals and Applications, Wiley-Interscience, New York, 1989.
[2] E. Pelizzetti, M. Schiavello, Photochemical Conversion and Storage of Solar Energy, Kluwer, Dordrecht, 1991.
[3] D.F. Ollis, H. Al-Ekabi (Eds.), Photocatalytic Purification and a Treatment of Water and Air, Elsevier, Amsterdam, 1993.
[4] L. Tinucci, E. Borgarello, C. Minero, E. Pelizzetti, in: D.F. Ollis, H. Al-Ekabi (Eds.), Photocatalytic Purification and Treatment of Water and Air, Elsevier, 1993.
[5] D. Bahnemann, J. Cunningham, M.A. Fox, E. Pelizzetti, P. Pichat, N. Serpone, in: D. Crosby, G. Hetz, R. Zepp (Eds.), Aquatic and Surface Photochemistry, Lewis Publishers, Boca Raton, FL, 1994, pp. 261–316.

[6] F.F. Fan, Y. Lin, A.J. Bard, J. Phys. Chem. 89 (1985) 448.
[7] H. Al-Ekabi, N. Serpone, J. Phys. Chem. 92 (1988) 5726.
[8] T. Tennakone, C.T.K. Tilakaratne, I.R.M. Kottegoda, J. Photochem. Photobiol. A Chem. 87 (1995) 1777.
[9] R.F.P. Nogueira, W.F. Jardin, J. Chem. Edu. 70 (1993) 861.
[10] Technical Bulletin No. 56, Degussa Canada, 4261 Mainway Drive, Burlington, Oct. 1982.
[11] R. Sargent, W.M. Rieman II, Anal. Chim. Acta 14 (1956) 381–385.
[12] H. Kawaguchi, Environ. Technol. Lett. 5 (1984) 471.
[13] M.R. Dhananjeyan, R. Annapoorani, S. Lakshmi, R. Renganathan, J. Photochem. Photobiol. A Chem. 96 (1996) 187.
[14] D. Duonghong, J. Ramsden, M. Grätzel, J. Am. Chem. Soc. 104 (1982) 2977.
[15] G.D. Parfitt, Prog. Surf. Membr. Sci. II (1976) 181.
[16] J. Augustynski, Structure and Bonding, Vol. 69, Springer-Verlag, Berlin, 1988.
[17] H.P. Boehm, M. Herrmann, Z. Anorg. Chem. 352 (1967) 156.
[18] A. Bard (Ed.), Encyclopedia of Electrochemistry of Elements, Vol. 2, Dekker, New York, 1974, p. 192.
[19] C.S. Turchi, D.F. Ollis, J. Catal. 122 (1990) 178.
[20] D.F. Ollis, C. Budiman, C. Lee, J. Catal. 88 (1984) 89.
[21] R. Matthews, J. Catal. III (1988) 264.
[22] L. Pruden, D. Ollis, J. Catal. 82 (1983) 404.
[23] G. Rothenberg, J. Moser, M. Gratzel, N. Serpone, D.K. Sharma, J. Am. Chem. Soc. 107 (1985) 8054.